AGU PUBLICATIONS

Geophysical Research Letters

RESEARCH LETTER
10.1002/2017GL074939

Key Points:
- A new approach to calculating the critical nucleation length for accelerating frictional slip is developed
- Differences compared to existing estimates are highlighted and predictions for bimaterial interfaces and finite-size systems are presented
- Comparison of the theoretical predictions to Finite-Element-Method calculations demonstrates favorable agreement

Supporting Information:
- Supporting Information S1

Correspondence to:
E. Bouchbinder,
eran.bouchbinder@weizmann.ac.il

Citation:
Aldam, M., Weikamp, M., Spatschek, R., Brener, E. A., & Bouchbinder, E. (2017). Critical nucleation length for accelerating frictional slip. *Geophysical Research Letters*, *44*, 11,390–11,398. https://doi.org/10.1002/2017GL074939

Received 13 JUL 2017
Accepted 24 OCT 2017
Accepted article online 2 NOV 2017
Published online 29 NOV 2017

Critical Nucleation Length for Accelerating Frictional Slip

Michael Aldam[1], Marc Weikamp[2], Robert Spatschek[2], Efim A. Brener[3], and Eran Bouchbinder[1]

[1]Chemical Physics Department, Weizmann Institute of Science, Rehovot, Israel, [2]Institute for Energy and Climate Research, Forschungszentrum Jülich, Jülich, Germany, [3]Peter Grünberg Institut, Forschungszentrum Jülich, Jülich, Germany

Abstract The spontaneous nucleation of accelerating slip along slowly driven frictional interfaces is central to a broad range of geophysical, physical, and engineering systems, with particularly far-reaching implications for earthquake physics. A common approach to this problem associates nucleation with an instability of an expanding creep patch upon surpassing a critical length L_c. The critical nucleation length L_c is conventionally obtained from a spring-block linear stability analysis extended to interfaces separating elastically deformable bodies using model-dependent fracture mechanics estimates. We propose an alternative approach in which the critical nucleation length is obtained from a related linear stability analysis of homogeneous sliding along interfaces separating elastically deformable bodies. For elastically identical half-spaces and rate-and-state friction, the two approaches are shown to yield L_c that features the same scaling structure, but with substantially different numerical prefactors, resulting in a significantly larger L_c in our approach. The proposed approach is also shown to be naturally applicable to finite-size systems and bimaterial interfaces, for which various analytic results are derived. To quantitatively test the proposed approach, we performed inertial Finite-Element-Method calculations for a finite-size two-dimensional elastically deformable body in rate-and-state frictional contact with a rigid body under sideway loading. We show that the theoretically predicted L_c and its finite-size dependence are in reasonably good quantitative agreement with the full numerical solutions, lending support to the proposed approach. These results offer a theoretical framework for predicting rapid slip nucleation along frictional interfaces.

1. Introduction

The process of rupture nucleation in which slowly driven frictional interfaces (faults) spontaneously develop elastodynamically propagating fronts accompanied by rapid slip is of fundamental importance for various fields, with far-reaching implications for earthquake physics. Quantitatively understanding the nucleation process is essential for predicting the dynamics of frictional interfaces in general and for earthquake dynamics in particular. There exists some observational evidence, based on seismological records (Harris, 2017; Ohnaka, 2000; Scholz, 1998), and some experimental evidence, based on laboratory measurements (Dieterich, 1979; Kato et al., 1992; Latour et al., 2013; McLaskey & Kilgore, 2013; Ohnaka & Kuwahara, 1990), which suggest that rapid rupture propagation accompanied by a marked seismological signature is preceded by precursory aseismic slip. This precursory aseismic slip is commonly associated with a slowly expanding creep patch defined as a slipping segment of finite linear size $L(t)$, embedded within a nonslipping fault. Accelerating slip is expected to emerge once $L(t)$ surpasses a critical nucleation length L_c. We note that other nucleation scenarios have been considered in the literature, see, for example, Ben-Zion (2008), but are not discussed here.

Various theoretical and computational works have indicated that the nucleation of accelerating slip is related to a frictional instability (Ben-Zion, 2001, 2008; Ben-Zion & Rice, 1997; Kaneko & Lapusta, 2008; Kaneko et al., 2016; Lapusta & Rice, 2003; Ruina, 1983; Scholz, 1998; Uenishi & Rice, 2003; Yamashita & Ohnaka, 1991). From this perspective, the critical nucleation length L_c corresponds to the critical conditions for the onset of instability that leads to accelerating slip and to the spontaneous propagation of elastodynamic rupture fronts. A major challenge is to understand the relations between the critical instability conditions and L_c. In this letter, we propose a theoretical approach for predicting L_c which differs from the conventional approach.

The conventional approach, based on a single degree of freedom spring-block analysis extended to deformable bodies using various model-dependent fracture mechanics estimates, is discussed in the

framework of rate-and-state constitutive laws in section 2. Our approach, based on the stability of homogeneous sliding of elastically deformable bodies, is introduced in section 3 and is shown to yield a significantly larger L_c for elastically identical half-spaces and rate-and-state friction. In section 4 we show that the proposed approach is naturally applicable to bimaterial interfaces, which are of great interest in various contexts (Adams, 2001; Aldam et al., 2017; Allam et al., 2014; Ampuero & Ben-Zion, 2008; Andrews & Ben-Zion, 1997; Ben-Zion, 2001; Ben-Zion & Andrews, 1998; Brener et al., 2016; Cochard & Rice, 2000; Gerde & Marder, 2001; Ranjith & Rice, 2001; Rice et al., 2001; Rubin & Ampuero, 2007; Shi & Ben-Zion, 2006; Weertman, 1980), and derive analytic results for L_c in this case, indicating that the bimaterial effect decreases L_c compared to available predictions in the literature. Finally, in section 5 we show that the proposed approach is applicable to finite-size systems and test our predictions against inertial Finite-Element-Method calculations for a finite-size two-dimensional elastically deformable body in rate-and-state frictional contact with a rigid body under sideway loading. The theoretically predicted L_c and its finite-size dependence are shown to be in reasonably good quantitative agreement with the full numerical solutions, lending support to the proposed approach. Section 6 offers some concluding remarks and discusses some prospects.

2. A Conventional Approach to Calculating the Nucleation Length L_c

As stated, the most prevalent approach to the nucleation of rapid slip at frictional interfaces associates nucleation with an instability of a slowly expanding creep patch. The creep patch features a nonuniform spatial distribution of slip velocity, in the quasi-static regime (where inertia and acoustic radiation are negligible), due to some external loading. It is assumed to be stable as long as its length $L(t)$ is smaller than a critical nucleation length L_c. When $L(t) = L_c$, the patch becomes unstable and transforms into a rupture front, accompanied by accelerated slip and dynamic propagation (where inertia and significant acoustic radiation are involved). As creep patches are nonstationary objects that involve spatially varying fields, determining their stability—and hence L_c—is a nontrivial challenge that typically requires invoking some approximations.

The most common approximation proceeds in two steps (Dieterich, 1986, 1992; Kaneko and Lapusta, 2008; Lapusta et al., 2000). First, the creep patch and the two elastically deformable bodies that form the frictional interface are replaced by a rigid block of mass M in contact with a rigid substrate and attached to a Hookean spring of stiffness K. That is, all of the spatial aspects of the problem are first neglected. The external loading and the typical slip velocity within the patch are mimicked by constantly pulling the Hookean spring at a velocity V. The rigid block is pressed against the rigid substrate by a normal force F_N, which gives rise to a frictional resistance force fF_N, where f is described by the friction law, which may depend on the block's slip $u(t)$, its time derivatives and the state of the frictional interface.

This single degree of freedom spring-block system is described by the force balance equation $M\ddot{u}(t) = K(Vt - u(t)) - f(\ldots)F_N$, where each superimposed dot denotes a time derivative. We assume that $f(\ldots)$ can be described by the rate-and-state constitutive framework, where $f(\dot{u}(t), \phi(t))$ is a function of the slip velocity $\dot{u}$ and of an internal state variable ϕ. The latter, which quantifies the typical age/maturity of contact asperities, evolves according to $\dot{\phi} = g(\phi\,\dot{u}/D)$, where D is a memory length scale and the function $g(\Omega)$ satisfies $g(1) = 0$ and $g'(1) < 0$. For example, two popular choices, that is, $g(\Omega) = 1 - \Omega$ (Baumberger & Caroli, 2006; Bhattacharya & Rubin, 2014; Marone, 1998; Nakatani, 2001; Ruina, 1983) and $g(\Omega) = -\Omega \log \Omega$ (Bhattacharya & Rubin, 2014; Gu et al., 1984; Ruina, 1983), feature $g'(1) = -1$.

Consider then a steady sliding state at a constant driving velocity $\dot{u} = V$ such that $\phi = D/V$. A standard linear stability analysis implies that this steady state becomes unstable if (Baumberger & Caroli, 2006; Bhattacharya & Rubin, 2014; Gu et al., 1984; Lapusta et al., 2000; Rice & Ruina, 1983; Ruina, 1983)

$$K < K_c \equiv \frac{\mathrm{d}f(V, D/V)}{\mathrm{d}\log V}\frac{g'(1)\,F_N}{D}\,, \tag{1}$$

where an inertial term proportional to MV^2 has been neglected. That is, an instability is predicted when the spring stiffness K is smaller than a critical stiffness K_c. Note that since generically $g'(1) < 0$, a necessary condition for instability is $\mathrm{d}f(V, D/V)/\mathrm{d}V < 0$, that is, that the sliding velocity V belongs to the velocity-weakening branch of the steady state friction curve (Ruina, 1983).

In the second step, the analysis is extended to spatially varying fields and elastically deformable bodies—relevant to realistic creep patches—by identifying the spring stiffness K in the spring-block system with

an L-dependent effective stiffness $K^{\text{eff}}(L)$ in the spatially varying and elastically deformable system. This is typically done through some fracture mechanics estimates which yield (Dieterich, 1986; Rice, 1993)

$$K^{\text{eff}}(L) = \eta \frac{\mu A_n}{L}, \tag{2}$$

where μ is the shear modulus, A_n is the nominal contact area, and the dimensionless number η is a model-dependent prefactor. As expected physically, the effective stiffness of the overall system, K^{eff}, is a decreasing function of the length of the creep patch, L. Using then $K^{\text{eff}} < K_c$ of equation (1) as an instability criterion, one obtains

$$L > L_c \equiv \eta \frac{\mu D}{\frac{\mathrm{d}f(V,D/V)}{\mathrm{d}\log V} g'(1)\,\sigma_0}, \tag{3}$$

where $\sigma_0 = F_N/A_n$. The numerical prefactor η is model dependent (e.g., it depends on the crack configuration, dimensionality, and loading configuration), and its value varies between $2/\pi$ and $4/3$ in the available literature (Dieterich, 1992, see Table 1). The nucleation criterion in equation (3), with η close to unity, is widely used in the literature, though we are not aware of computational or experimental studies that quantitatively and systematically tested it. Next, we present a different approach for calculating L_c.

3. An Approach Based On the Stability of Homogeneous Sliding of Elastically Deformable Bodies

Our goal here is to propose an alternative approach to calculating the critical nucleation length L_c. In the proposed approach, nucleation is viewed as a spatiotemporal instability occurring along the creep patch which is assumed to be stable from the fracture mechanics perspective, that is, to propagate under stable Griffith energy balance conditions (Freund, 1990). Since, in general, an elastic body can be thought of as a scale-dependent spring, one expects short wavelength λ (large wave number $k = 2\pi/\lambda$) perturbations to be stable and instability—if it exists—to emerge beyond a critical (minimal) wavelength λ_c (i.e., below a critical wave number k_c). Consequently, when the size $L(t)$ of the expanding creep patch is small, $L(t) < 2\pi/k_c$, we expect it to be stable. A loss of stability is expected when an unstable perturbation can *first* fit into the creep patch, that is, when the patch size satisfies $L(t) = L_c \equiv 2\pi/k_c$.

In this physical picture, the major goal is to calculate the critical wave number k_c. There is, however, no unique and general procedure to study the stability of nonstationary (time dependent) and spatially varying solutions such as those associated with an expanding creep patch. Consequently, we invoke an approximation in which the spatially varying slip velocity within the creep patch is replaced by a homogeneous (space-independent) characteristic slip velocity V. With this approximation in mind, we need to study the stability of steady state homogeneous sliding of an infinitely long system (in the sliding direction) in order to calculate k_c. Applying the result to the actual creep patch, accelerating slip nucleation is predicted to occur when $L(t) = L_c \equiv 2\pi/k_c$. This idea has been introduced, pursued, and substantiated in the context of thin layers sliding on top of rigid substrates in Bar-Sinai et al. (2013). Our aim here is to significantly generalize the idea to any frictional system.

We consider a long elastic body in the x direction of height $H^{(1)}$ in the y direction steadily sliding with a relative slip velocity V on top of a long elastic body of height $H^{(2)}$. The bodies may be made of different elastic materials and are pressed one against the other by a normal stress σ_0, see Figure 1 (left). As we are interested in the response of the system to spatiotemporal perturbations on top of the homogeneous sliding state at a velocity V, we define the slip displacement $\epsilon(x,t) \equiv u_x(x, y = 0^+, t) - u_x(x, y = 0^-, t)$ and the slip velocity $v(x,t) \equiv \dot{\epsilon}(x,t)$, where $\boldsymbol{u}(x,y,t)$ is the displacement field and $y = 0$ is the fault plane (the superscript $+/-$ means approaching the fault plane from the upper/lower body side, respectively). $\boldsymbol{u}(x,y,t)$ for each body satisfies the Navier-Lamé equation $\nabla\cdot\boldsymbol{\sigma} = \frac{\mu}{1-2\nu}\nabla(\nabla\cdot\boldsymbol{u}) + \mu\nabla^2\boldsymbol{u} = \rho\,\ddot{\boldsymbol{u}}$, with its own shear modulus μ, Poisson's ratio ν, and mass density ρ (Landau & Lifshitz, 1986). The Cauchy stress tensor field $\boldsymbol{\sigma}$ was related to the displacement field $\boldsymbol{u}$ through Hooke's law, and each superimposed dot represents a partial time derivative.

The fault at $y = 0$ is assumed to be described by the rate-and-state constitutive relation $\tau = \sigma_{xy} = -f(v,\phi)\sigma_{yy}$. Fault opening or interpenetration are excluded; that is, we assume $u_y(x, y = 0^+, t) = u_y(x, y = 0^-, t)$, and σ_{xy} and σ_{yy} are continuous across the fault. The internal state field $\phi(x,t)$ evolves according to $\dot{\phi} = g(\phi\,\dot{u}/D)$, with $g(1) = 0$ and $g'(1) < 0$, as in section 2. We then introduce interfacial slip perturbations of the form $\delta\epsilon \propto \exp(\Lambda t - ikx)$, where Λ is the complex growth rate and k is the wave number. The shear and normal

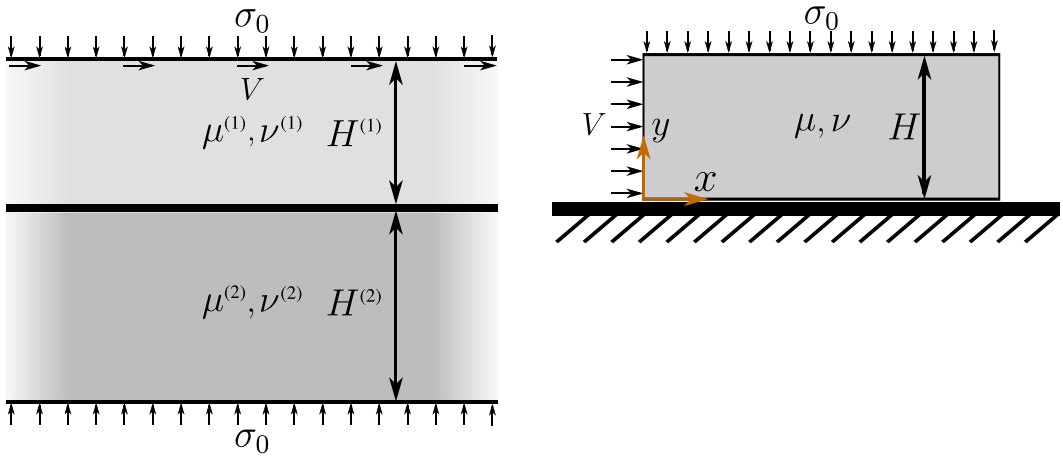

Figure 1. (left) A long elastic body of height $H^{(1)}$, shear modulus $\mu^{(1)}$, and Poisson's ratio $\nu^{(1)}$ sliding on top of another long elastic body of height $H^{(2)}$, shear modulus $\mu^{(2)}$, and Poisson's ratio $\nu^{(2)}$. The color gradients represent the fact that the bodies are essentially infinitely long. The bodies are pressed one against the other by a normal stress of magnitude σ_0 and a homogeneous sliding state at a relative velocity V (in the figure the lower body is assumed to be stationary) is reached by the application of a shear stress of magnitude τ_0 to the top and bottom edges (not shown). (right) The same as in Figure 1 (left) except that the lower body is infinitely rigid, $\mu^{(2)} \to \infty$, the upper body is of finite length, and the velocity V is applied to the lateral edge at $x = 0$. Note that the superscript (1) is unnecessary here and hence is omitted.

stress perturbations are related to $\delta\epsilon$ using the solution of the quasi-static Navier-Lamé equation and take the form $\delta\sigma_{xy} = -\mu\, k\, G_1\, \delta\epsilon$, $\delta\sigma_{yy} = i\mu\, k\, G_2\, \delta\epsilon$; μ is the shear modulus of the upper body. We focus on the quasi-static regime, that is, excluding inertia, because nucleation generically takes place in this regime. The quasi-static elastic transfer functions G_1 and G_2, see supporting information (Geubelle & Rice, 1995), contain all of the information about the system's geometry, the elastic properties of the sliding bodies, and loading conditions (e.g., velocity versus stress boundary condition). The perturbation in the frictional resistance takes the form $\delta f = \frac{\Lambda(a\Lambda\ell - \zeta V)}{V(V+\Lambda\ell)}\,\delta\epsilon$, where we used $\delta v = \Lambda\delta\epsilon$, and the definitions $\ell \equiv -\frac{D}{g'(1)} > 0$, $a \equiv v\frac{\partial f(v,\phi)}{\partial v} > 0$ and $\zeta \equiv -v\frac{\mathrm{d}f(v,D/v)}{\mathrm{d}v} = -\frac{\mathrm{d}f(v,D/v)}{\mathrm{d}\log v}$ (the latter two are evaluated at $v = V$); see supporting information. Note that ζ can be both positive (velocity-weakening friction) and negative (velocity-strengthening friction) depending on the materials, the sliding velocity V, and physical conditions (e.g., temperature) (Bar-Sinai et al., 2014). For the small slip velocities regime of interest here we assume that friction is velocity weakening; hence, we consider $\zeta > 0$.

The linear perturbation spectrum $\Lambda(k)$ is determined by the perturbation of the constitutive relation, which reads

$$\delta\tau = \delta\sigma_{xy} = \sigma_0\delta f - f\delta\sigma_{yy}\,. \tag{4}$$

Substituting the results for $\delta\sigma_{xy}$, $\delta\sigma_{yy}$, and δf, we obtain an equation for $\Lambda(k)$

$$\mu\, k\left(G_1 - ifG_2\right) + \sigma_0\frac{\Lambda(a\Lambda\ell - \zeta V)}{V(V+\Lambda\ell)} = 0\,. \tag{5}$$

Once solutions $\Lambda(k)$ are obtained, instability is implied whenever $\Re[\Lambda(k)] > 0$, corresponding to an exponential growth of perturbations. Consequently, k_c is determined as the largest wave number k (smallest wavelength) for which $\Re[\Lambda(k)] = 0$ and the critical nucleation length is estimated as $L_c \equiv 2\pi/k_c$.

Solutions to equation (5) for some cases are available in the literature. Most notably, for two identical half-spaces, we have $G_1 = \mathrm{sign}(k)[2(1-\nu)]^{-1}$ and $G_2 = 0$ (see supporting information), where the latter represents the absence of a bimaterial effect for elastically identical materials of the same shape/geometry. Plugging these transfer functions into equation (5), one can readily obtain a known result for the critical wave number (Rice & Ruina, 1983), which reads $k_c = 2(1-\nu)\zeta\sigma_0\mu^{-1}\ell^{-1}$. Using our proposed criterion $L_c \equiv 2\pi/k_c$, we obtain

$$L_c = \frac{\pi\,\mu\,\ell}{\zeta(1-\nu)\sigma_0} \qquad \Longrightarrow \qquad \eta = \frac{\pi}{1-\nu}\,, \tag{6}$$

where η was defined in equation (3). This prediction for the critical nucleation length is identical to the one in equation (3), which basically follows from dimensional considerations, once the prefactor $\eta = \pi(1-\nu)^{-1}$ is identified as done above (and the definitions of ℓ and ζ are recalled). This value of the prefactor η is π times larger than the largest value we have been able to trace in the available literature based on the conventional approach; hence, we conclude that the proposed approach predicts a significantly larger nucleation length L_c for identical half-spaces as compared to the conventional approach. Indeed, some numerical simulations of earthquake nucleation indicated that the conventional prediction with $\eta \simeq 1$ quite significantly underestimates the observed L_c (Lapusta & Rice, 2003).

The physical picture of nucleation developed in this section suggests that the *origin* of nucleation is a linear frictional instability, while the *outcome* of nucleation is typically strongly nonlinear. In particular, the critical nucleation conditions coincide with the onset of linear instability when the patch size reaches L_c, then the slip velocity increases exponentially in the linear regime until nonlinearities set in when the slip velocity is large enough. Finally, the patch breaks up into propagating rupture fronts. The linear stage of the instability is expected to be rather generic, and in particular nearly independent of the exact functional form of $g(\cdot)$ (with $g(1) = 0$ and $g'(1) < 0$) within the rate-and-state constitutive framework and of the background strength of the fault quantified by the initial age $\phi(t = 0)$, while the nonlinear stages that follow may depend on the details of the constitutive relation and the background fault strength.

These generic properties of the onset of nucleation will be explicitly demonstrated in section 5 below. Furthermore, we note that the works of Rubin and Ampuero (2005) and Ampuero and Rubin (2008) apparently focus on the nonlinear stages of nucleation, which is consistent with the fact that they find differences between different friction laws and that their patches can shrink/expand during the nonlinear evolution of the instability. The nonlinear stages—on the route to rupture propagation—cannot take place, though, if the patch does not reach first the size L_c determined by the linear instability. Hence, we believe that the above defined L_c is the relevant nucleation length, and not any other length that might characterize the nonlinear evolution of the instability.

4. Application to Bimaterial Interfaces

The general framework laid down in the previous section, unlike the conventional approach, can be naturally applied to bimaterial interfaces. We consider then two half-spaces made of different elastic materials: the upper half-space is characterized by a shear modulus $\mu^{(1)}$ and Poisson's ratio $\nu^{(1)}$ and the lower half-space by a shear modulus $\mu^{(2)}$ and Poisson's ratio $\nu^{(2)}$. It corresponds to Figure 1 (left), once the limits $H^{(1)} \to \infty$ and $H^{(2)} \to \infty$ are taken. Defining $\psi \equiv \mu^{(2)}/\mu^{(1)}$ and $\mu \equiv \mu^{(1)}$ (i.e., the shear modulus of the upper body is denoted by μ, as before), the elastic transfer functions for this bimaterial system take the form (Rice et al., 2001) (see also supporting information)

$$G_1 = \frac{\mathcal{M}}{2\mu}\mathrm{sign}(k), \qquad G_2 = \frac{\beta\mathcal{M}}{2\mu}, \tag{7}$$

where

$$\mathcal{M} \equiv \frac{2\psi\mu(1-\beta^2)^{-1}}{\psi(1-\nu^{(1)})+(1-\nu^{(2)})}, \qquad \beta \equiv \frac{\psi(1-2\nu^{(1)})-(1-2\nu^{(2)})}{2[\psi(1-\nu^{(1)})+(1-\nu^{(2)})]}. \tag{8}$$

$\mathcal{M}$ plays the role of an effective bimaterial modulus, which approaches $\mu/(1-\nu)$ in the identical materials limit, $\mu^{(1)} = \mu^{(2)} = \mu$, and $\nu^{(1)} = \nu^{(2)} = \nu$. β, which appears in G_2 but not in G_1, vanishes in the identical materials limit (and consequently G_2 vanishes in this limit as well), and hence, it quantifies the bimaterial effect.

The presence of a bimaterial contrast, $\beta \neq 0$, introduces a new destabilization effect associated with a coupling between slip and normal stress perturbations, in addition to the destabilizing effect associated with velocity-weakening friction, $\zeta > 0$. Hence, on physical grounds one expects L_c to decrease with increasing bimaterial contrast. To test this, we insert $G_{1,2}$ of equation (7) into equation (5) and calculate k_c, obtaining the following expression for $L_c = 2\pi/k_c$

$$L_c = \frac{\pi\mathcal{M}\ell}{\zeta\sigma_0}\frac{(f\beta)^2\left(1+\zeta/a-\sqrt{(1+\zeta/a)^2+\frac{4\zeta/a}{(f\beta)^2}}\right)+2\zeta/a}{2\zeta/a}. \tag{9}$$

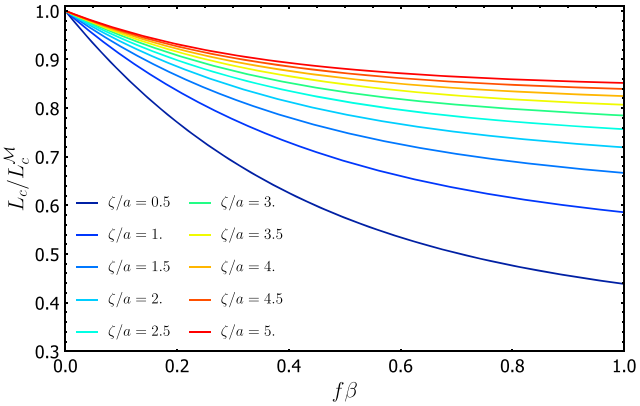

Figure 2. The critical nucleation length L_c (normalized by $L_c^{\mathcal{M}}$) for bimaterial interfaces separating two half-spaces, cf. equation (9), plotted as a function of $f\beta$ for various values of ζ/a.

The first multiplicative contribution on the right-hand side, $L_c^{\mathcal{M}} \equiv \frac{\pi\mathcal{M}\ell}{\zeta\sigma_0}$, is obtained by replacing $\mu/(1-\nu)$ in our result in equation (6) by the effective modulus $\mathcal{M}$. A similar replacement has been proposed by Rubin and Ampuero (2007) in the context of a different heuristic estimate of the critical nucleation length for bimaterial interfaces. Consequently, we plot in Figure 2 L_c of equation (9), normalized by $L_c^{\mathcal{M}}$, as a function of $f\beta$ for various values of ζ/a. It is observed that L_c for bimaterial interfaces is generically *smaller* than the conventional estimate $L_c^{\mathcal{M}}$, indicating that bimaterial interfaces may be more unstable than previously considered. We note in passing that equation (9) remains valid also in the presence of velocity-strengthening friction, $\zeta < 0$, for which it predicts that for sufficiently strong bimaterial contrasts, $f\beta \geq \frac{2\sqrt{-a\zeta}}{a+\zeta}$, instability is implied even for velocity-strengthening friction (Rice et al., 2001).

5. Application to Finite-Size Systems and Comparison to Inertial Finite-Element-Method Calculations

The general framework laid down in section 3, unlike the conventional approach, can be naturally applied to finite-size systems. To demonstrate this, we consider here a system that features both finite dimensions and a bimaterial contrast. In particular, we consider a long deformable body of height H, and of elastic constants μ and ν, in rate-and-state frictional contact with a rigid substrate under the application of a compressive stress σ_0 and a shear stress τ_0. This configuration corresponds to Figure 1 (left), once the limit $\mu^{(2)} \to \infty$ is taken. In this case, the elastic transfer functions appearing in equation (5) take the form (see supporting information)

$$G_1 = \frac{4(1-\nu)(2Hk + \sinh(2Hk))}{2H^2k^2 + (3-4\nu)\cosh(2Hk) - 4\nu(3-2\nu) + 5}\,,$$
$$G_2 = \frac{4\left(H^2k^2 + (1-2\nu)\sinh^2(Hk)\right)}{2H^2k^2 + (3-4\nu)\cosh(2Hk) - 4\nu(3-2\nu) + 5}\,. \tag{10}$$

When substituted in equation (5), we obtain a complex equation which is not analytically tractable, but rather is amenable to numerical analysis. Let us denote the solution by $k_c(H)$ and the corresponding prediction for the critical nucleation length by $L_c(H) = 2\pi/k_c(H)$.

Equation (5), with $G_{1,2}$ of equation (10), does admit an analytic solution in the limit $Hk \to 0$, that is, when the system height H is small compared to field variations parallel to the interface characterized by a length scale $\sim k^{-1}$. In this limit, we find $G_1 \simeq 2Hk(1-\nu)^{-1}$ and $G_2 \simeq 0$. Using these in equation (5), we obtain

$$L_c^{(Hk\to 0)} \simeq 2\pi\sqrt{\frac{2H\mu\,\ell}{\zeta(1-\nu)\sigma_0}}\,. \tag{11}$$

$L_c^{(Hk\to 0)}$ predicts the small H behavior of $L_c(H)$ and constrains any numerical calculation of $L_c(H)$ to be quantitatively consistent with it in this limit. In addition, it is fully consistent with the results of Bar-Sinai et al. (2013). We numerically calculated $L_c(H)$ for the following set of parameters: $\mu = 3.1$ GPa, $\nu = 1/3$, $f = 0.41$, $a = 0.0068$, $\zeta = 0.016$, $\sigma_0 = 1$ MPa, $\ell = 0.5\,\mu$m, and $V = 10\,\mu$m/s (the latter corresponds to an applied shear stress $\tau_0 = f(V, \phi = D/V)\sigma_0$). The result is plotted in the main panel of Figure 3 (solid line). When $L_c^{(Hk\to 0)}$ of equation (11) is superimposed on it (dashed line), perfect agreement at small H and significant deviations at larger H are observed, as expected.

Our goal now is to quantitatively test the ability of the calculated $L_c(H)$ to predict the critical nucleation length in a realistic situation in which a slowly expanding creep patch spontaneously nucleates accelerating slip. We would also like to test the theoretical prediction that L_c is nearly independent of the specific friction law (in particular the aging versus the slip ϕ evolution laws) and the background fault strength (the initial value of ϕ). To these aims, we performed inertial Finite-Element-Method (FEM) calculations that are directly relevant for the geometrical configuration and material parameters discussed in the last two paragraphs. In particular,

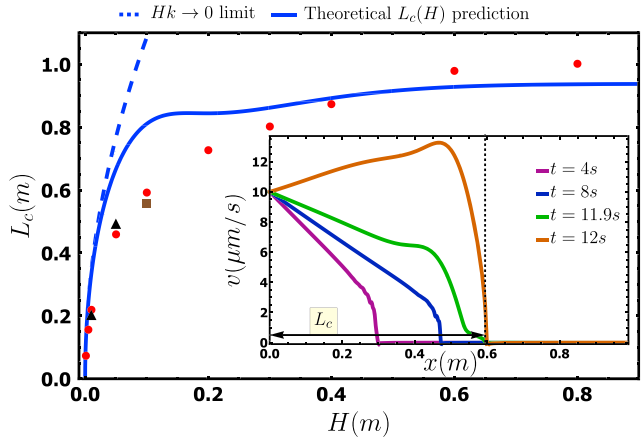

Figure 3. The theoretical prediction for the critical nucleation length L_c for a generic rate-and-state constitutive relation as a function of the height H of an elastic body sliding on top of a rigid substrate (solid line). The material, interfacial, and loading parameters are given in the text. The analytic approximation for $L_c(H)$ in the $Hk \to 0$ limit, cf. equation (11), is added (dashed line). The nucleation length measured in inertial FEM simulations of a finite elastic body of height H under sideway loading for the aging law (see text and Figure 1 (right) for details) is shown as a function of H (red circles). For $H = 0.01$ m and $H = 0.05$ m, L_c for the slip law is also shown (black triangles), demonstrating small variation compared to the result for the aging law. For $H = 0.1$ m, L_c for $\phi(t = 0) = 10^3$ s is also shown (brown square), demonstrating small variation compared to the result for $\phi(t = 0) = 1$ s (i.e., 3 orders of magnitude difference in the initial age of the fault). (inset) A sequence of snapshots in time (see legend) of the slip velocity field in inertial FEM simulations for the aging law with $H = 0.1$ m, demonstrating the propagation of a creep patch from the loading edge at $x = 0$ into the interface. At a certain creep patch length (denoted by a vertical dashed line and a horizontal double-head arrow) an instability accompanied by accelerated slip takes place. This is the numerically extracted nucleation length for this height H, as can be seen in the main panel.

we consider a deformable body of height H which is also of finite extent in the direction parallel to the interface and which is loaded (by an imposed velocity $V = 10$ μm/s that is initiated at $t = 0$) at its lateral edge (defined as $x = 0$), rather than at its top edge at $y = H$; see Figure 1 (right). The advantage of this sideway loading configuration is that it naturally generates a creep patch that slowly expands from $x = 0$ along the interface, cf. the inset of Figure 3. The interface is first described by the aging rate-and-state constitutive relation with $\dot{\phi} \simeq 1 - \phi v/D$ and $f(v, \phi) \simeq f_0 + a \log(v/V) + (\zeta + a) \log(\phi V/D)$, where $f_0 = 0.41$ and the other parameters are as above. The initial conditions are $v(t = 0) = 0$ and $\phi(t = 0) = 1s$. The full constitutive relation used in the FEM calculations, which also allows a transition from stick ($v = 0$) to slip ($v > 0$), can be found in the supporting information (Hecht, 2012).

Our theoretical approach predicts that the creep patch loses its stability and develops accelerating slip upon reaching a certain critical length. This is indeed observed in the inset of Figure 3, where the slip velocity blows up when the creep patch reaches a certain length. We then measured the critical length in inertial FEM calculations for different system heights H (in addition to the inset of Figure 3, see also the supporting information for the details of the determination of L_c in the numerical calculations) and superimposed the results for the aging law (red circles) on the main panel of Figure 3. It is observed that the theoretical prediction for the critical nucleation length $L_c(H)$ is in reasonably good quantitative agreement with the FEM results for the full range of system heights H. This major result lends serious support to the approach developed in this letter.

In order to test whether the theoretically predicted critical nucleation length $L_c(H)$ is indeed nearly independent of the details of the friction law, we repeated the above described FEM calculations for $H = 0.01$ m and $H = 0.05$ m with the slip law instead of the aging law; that is, we used for the slip law $\dot{\phi} \simeq -(\phi v/D) \log(\phi v/D)$ (the full constitutive relation can again be found in the supporting information). The resulting critical nucleation length (black triangles in main panel of Figure 3) for both H values exhibits only a small variation (less than 10%) compared to the results for the aging law. Furthermore, we repeated the above described FEM calculations for the aging law with $H = 0.1$ m, except that we increased the initial age of the fault by 3 orders of magnitude, from $\phi(t = 0) = 1$ s to $\phi(t = 0) = 10^3$ s. The resulting critical nucleation length (brown square in main panel of Figure 3) exhibits only a small variation (less than 10%) compared to the result for $\phi(t = 0) = 1$ s. These results lend strong support to the idea that the critical nucleation length L_c is determined by a linear instability that is reasonably predicted by the procedure developed in this Letter.

6. Concluding Remarks

In this letter we developed a theoretical approach for the calculation of the critical nucleation length for accelerating slip L_c. The proposed approach builds on existing literature by adopting the view that nucleation is associated with a linear frictional instability of an expanding creep patch. It deviates from the conventional approach in the literature by replacing the problem of the stability of a spatiotemporally varying creep patch by an effective homogeneous sliding linear stability analysis for deformable bodies, rather than invoking a spring-block stability analysis supplemented with some fracture mechanics estimates for deformable bodies. The quality of the predictions emerging from the proposed approach therefore depend on the degree by which the creep patch can be approximated by spatially homogeneous fields. This approximation is expected to be reasonable in many cases in light of the weak/logarithmic velocity dependence of friction in many materials. The temporal aspects of the creep patch propagation are taken into account by the requirement that it becomes unstable upon attaining a length for which an unstable mode from the homogeneous linear stability analysis can be first fitted into.

The proposed approach is rather general and applies to a broad range of physical situations. For sliding along rate-and-state frictional interfaces separating identical elastic half-spaces, it has been shown to predict a significantly larger nucleation length compared to the conventional approach. For sliding along rate-and-state frictional interfaces separating different elastic half-spaces, the proposed approach has been shown to predict a bimaterial weakening effect which appears to be stronger than previously hypothesized, resulting in a smaller nucleation length. Finally, the proposed approach has been applied to finite-height systems. For this case, the scenario of a loss of stability of an expanding creep patch has been directly demonstrated using inertial FEM calculations and the predicted nucleation length has been shown to be in reasonably good quantitative agreement with direct FEM results for a range of system heights. The quality of the theoretical predictions has been shown to be nearly independent of the specific friction law used (aging versus slip laws) and the background strength of the fault. These results offer a theoretical framework for predicting rapid slip nucleation along faults and hence may give rise to better short-term earthquake prediction capabilities. The proposed approach can and should be quantitatively tested in a wide variety of interfacial rupture nucleation problems, using both theoretical tools and extensive numerical simulations.

Acknowledgments

E. B. acknowledges support from the Israel Science Foundation (grant 295/16), the William Z. and Eda Bess Novick Young Scientist Fund, COST Action MP1303, and the Harold Perlman Family. R. S. acknowledges support from the DFG priority program 1713. We are grateful to Eric Dunham, one of the reviewers of the manuscript, for his valuable and constructive comments and suggestions. We also thank Robert Viesca for useful discussions in the context of nucleation on bimaterial interfaces. M. A. acknowledges Yohai Bar-Sinai for helpful guidance and assistance. The analytical formulae and numerical methods described in the main text and supporting information are sufficient to reproduce all the results and plots presented in the paper.

References

Adams, G. G. (2001). An intersonic slip pulse at a frictional interface between dissimilar materials. *Journal of Applied Mechanics*, *68*(1), 81–86. https://doi.org/10.1115/1.1349119

Aldam, M., Xu, S., Brener, E. A., Ben-Zion, Y., & Bouchbinder, E. (2017). Non-monotonicity of the frictional bimaterial effect. *Journal of Geophysical Research: Solid Earth*, *122*. https://doi.org/10.1002/2017JB014665

Allam, A. A., Ben-Zion, Y., & Peng, Z. (2014). Seismic imaging of a bimaterial interface along the Hayward Fault, CA, with fault zone head waves and direct P arrivals. *Pure and Applied Geophysics*, *171*(11), 2993–3011. https://doi.org/10.1007/s00024-014-0784-0

Ampuero, J.-P., & Ben-Zion, Y. (2008). Cracks, pulses and macroscopic asymmetry of dynamic rupture on a bimaterial interface with velocity-weakening friction. *Geophysical Journal International*, *173*(2), 674–692. https://doi.org/10.1111/j.1365-246X.2008.03736.x

Ampuero, J.-P., & Rubin, A. M. (2008). Earthquake nucleation on rate and state faults—Aging and slip laws. *Journal of Geophysical Research: Solid Earth*, *113*, B01302. https://doi.org/10.1029/2007JB005082

Andrews, D. J., & Ben-Zion, Y. (1997). Wrinkle-like slip pulse on a fault between different materials. *Journal of Geophysical Research*, *102*(B1), 553–571. https://doi.org/10.1029/96JB02856

Bar-Sinai, Y., Spatschek, R., Brener, E. A., & Bouchbinder, E. (2013). Instabilities at frictional interfaces: Creep patches, nucleation, and rupture fronts. *Physical Review E*, *88*(6), 060403. https://doi.org/10.1103/PhysRevE.88.060403

Bar-Sinai, Y., Spatschek, R., Brener, E. A., & Bouchbinder, E. (2014). On the velocity-strengthening behavior of dry friction. *Journal of Geophysical Research: Solid Earth*, *119*, 1738–1748. https://doi.org/10.1002/2013JB010586

Baumberger, T., & Caroli, C. (2006). Solid friction from stick-slip down to pinning and aging. *Advances in Physics*, *55*(3–4), 279–348. https://doi.org/10.1080/00018730600732186

Ben-Zion, Y. (2001). Dynamic ruptures in recent models of earthquake faults. *Journal of the Mechanics and Physics of Solids*, *49*(9), 2209–2244. https://doi.org/10.1016/S0022-5096(01)00036-9

Ben-Zion, Y. (2008). Collective behavior of earthquakes and faults: Continuum-discrete transitions, progressive evolutionary changes, and different dynamic regimes. *Reviews of Geophysics*, *46*, RG4006. https://doi.org/10.1029/2008RG000260

Ben-Zion, Y., & Andrews, D. J. (1998). Properties and implications of dynamic rupture along a material interface. *Bulletin of the Seismological Society of America*, *88*(4), 1085–1094.

Ben-Zion, Y., & Rice, J. R. (1997). Dynamic simulations of slip on a smooth fault in an elastic solid. *Journal of Geophysical Research*, *102*(B8), 17,771–17,784. https://doi.org/10.1029/97JB01341

Bhattacharya, P., & Rubin, A. M. (2014). Frictional response to velocity steps and 1-D fault nucleation under a state evolution law with stressing-rate dependence. *Journal of Geophysical Research: Solid Earth*, *119*, 2272–2304. https://doi.org/10.1002/2013JB010671

Brener, E. A., Weikamp, M., Spatschek, R., Bar-Sinai, Y., & Bouchbinder, E. (2016). Dynamic instabilities of frictional sliding at a bimaterial interface. *Journal of the Mechanics and Physics of Solids*, *89*, 149–173. https://doi.org/10.1016/j.jmps.2016.01.009

Cochard, A., & Rice, J. R. (2000). Fault rupture between dissimilar materials: Ill-posedness, regularization, and slip-pulse response. *Journal of Geophysical Research*, *105*, 25,891–25,907. https://doi.org/10.1029/2000JB900230

Dieterich, J. H. (1979). Modeling of rock friction: 1. Experimental results and constitutive equations. *Journal of Geophysical Research*, *84*(B5), 2161–2168. https://doi.org/10.1029/JB084iB05p02161

Dieterich, J. H. (1986). A model for the nucleation of earthquake slip. In S. Das, J. Boatwright, & C. H. Scholz (Eds.), *Earthquake Source Mechanics* (pp. 37–47). Washington, DC: American Geophysical Union. https://doi.org/10.1029/GM037p0037

Dieterich, J. H. (1992). Earthquake nucleation on faults with rate-and state-dependent strength. *Tectonophysics*, *211*(1–4), 115–134. https://doi.org/10.1016/0040-1951(92)90055-B

Freund, L. B. (1990). *Dynamic fracture mechanics*. Cambridge: Cambridge University Press.

Gerde, E., & Marder, M. (2001). Friction and fracture. *Nature*, *413*(6853), 285–288. https://doi.org/10.1038/35095018

Gu, J.-C., Rice, J. R., Ruina, A. L., & Tse, S. T. (1984). Slip motion and stability of a single degree of freedom elastic system with rate and state dependent friction. *Journal of the Mechanics and Physics of Solids*, *32*(3), 167–196. https://doi.org/10.1016/0022-5096(84)90007-3

Geubelle, P., & Rice, J. R. (1995). A spectral method for three-dimensional elastodynamic fracture problems. *Journal of the Mechanics and Physics of Solids*, *43*(11), 1791–1824. https://doi.org/10.1016/0022-5096(95)00043-I

Harris, R. A. (2017). Large earthquakes and creeping faults. *Reviews of Geophysics*, *55*, 169–198. https://doi.org/10.1002/2016RG000539

Hecht, F. (2012). New development in FreeFem++. *Journal of Numerical Mathematics*, *20*(3–4), 251–266. https://doi.org/10.1515/jnum-2012-0013

Kaneko, Y., & Lapusta, N. (2008). Variability of earthquake nucleation in continuum models of rate-and-state faults and implications for aftershock rates. *Journal of Geophysical Research*, *113*, B12312. https://doi.org/10.1029/2007JB005154

Kaneko, Y., Nielsen, S. B., & Carpenter, B. M. (2016). The onset of laboratory earthquakes explained by nucleating rupture on a rate-and-state fault. *Journal of Geophysical Research: Solid Earth*, *121*, 6071–6091. https://doi.org/10.1002/2016JB013143

Kato, N., Yamamoto, K., Yamamoto, H., & Hirasawa, T. (1992). Strain-rate effect on frictional strength and the slip nucleation process. *Tectonophysics*, *211*(1–4), 269–282. https://doi.org/10.1016/0040-1951(92)90064-D

Landau, L., & Lifshitz, E. (1986). *Theory of elasticity* (3rd ed., Vol. 7). Oxford: (Course of Theoretical Physics) Butterworth-Heinemann.

Lapusta, N., & Rice, J. R. (2003). Nucleation and early seismic propagation of small and large events in a crustal earthquake model. *Journal of Geophysical Research: Solid Earth*, *108*(B4), 2205. https://doi.org/10.1029/2001JB000793

Lapusta, N., Rice, J. R., Ben-Zion, Y., & Zheng, G. (2000). Elastodynamic analysis for slow tectonic loading with spontaneous rupture episodes on faults with rate- and state-dependent friction. *Journal of Geophysical Research*, *105*(B10), 23,765–23,789. https://doi.org/10.1029/2000JB900250

Latour, S., Schubnel, A., Nielsen, S. B., Madariaga, R., & Vinciguerra, S. (2013). Characterization of nucleation during laboratory earthquakes. *Geophysical Research Letters*, *40*, 5064–5069. https://doi.org/10.1002/grl.50974

Marone, C. (1998). The effect of loading rate on static friction and the rate of fault healing during the earthquake cycle. *Nature*, *391*(6662), 69–72. https://doi.org/10.1038/34157

McLaskey, G. C., & Kilgore, B. D. (2013). Foreshocks during the nucleation of stick-slip instability. *Journal of Geophysical Research: Solid Earth*, *118*, 2982–2997. https://doi.org/10.1002/jgrb.50232

Nakatani, M. (2001). Conceptual and physical clarification of rate and state friction: Frictional sliding as a thermally activated rheology. *Journal of Geophysical Research*, *106*(B7), 13347–13380. https://doi.org/10.1029/2000JB900453

Ohnaka, M. (2000). A physical scaling relation between the size of an earthquake and its nucleation zone size. *Pure and Applied Geophysics*, *157*(11), 2259–2282. https://doi.org/10.1007/PL00001084

Ohnaka, M., & Kuwahara, Y. (1990). Characteristic features of local breakdown near a crack-tip in the transition zone from nucleation to unstable rupture during stick-slip shear failure. *Tectonophysics*, *175*(1–3), 197–220. https://doi.org/10.1016/0040-1951(90)90138-X

Ranjith, K., & Rice, J. R. (2001). Slip dynamics at an interface between dissimilar materials. *Journal of the Mechanics and Physics of Solids*, *49*(2), 341–361. https://doi.org/10.1016/S0022-5096(00)00029-6

Rice, J. R. (1993). Spatio-temporal complexity of slip on a fault. *Journal of Geophysical Research*, *98*(B6), 9885–9907. https://doi.org/10.1029/93JB00191

Rice, J. R., Lapusta, N., & Ranjith, K. (2001). Rate and state dependent friction and the stability of sliding between elastically deformable solids. *Journal of the Mechanics and Physics of Solids*, *49*(9), 1865–1898. https://doi.org/10.1016/S0022-5096(01)00042-4

Rice, J. R., & Ruina, A. L. (1983). Stability of steady frictional slipping. *Journal of Applied Mechanics*, *50*(2), 343–349. https://doi.org/10.1115/1.3167042

Rubin, A. M., & Ampuero, J.-P. (2005). Earthquake nucleation on (aging) rate and state faults. *Journal of Geophysical Research*, *110*, B11312. https://doi.org/10.1029/2005JB003686

Rubin, A. M., & Ampuero, J.-P. (2007). Aftershock asymmetry on a bimaterial interface. *Journal of Geophysical Research*, *112*, B05307. https://doi.org/10.1029/2006JB004337

Ruina, A. L. (1983). Slip instability and state variable friction laws. *Journal of Geophysical Research*, *88*, 10,359–10,370. https://doi.org/10.1029/JB088iB12p10359

Scholz, C. H. (1998). Earthquakes and friction laws. *Nature*, *391*(6662), 37–42. https://doi.org/10.1038/34097

Shi, Z., & Ben-Zion, Y. (2006). Dynamic rupture on a bimaterial interface governed by slip-weakening friction. *Geophysical Journal International*, *165*(2), 469–484. https://doi.org/10.1111/j.1365-246X.2006.02853.x

Uenishi, K., & Rice, J. R. (2003). Universal nucleation length for slip-weakening rupture instability under nonuniform fault loading. *Journal of Geophysical Research*, *108*, 2042. https://doi.org/10.1029/2001JB001681

Weertman, J. (1980). Unstable slippage across a fault that separates elastic media of different elastic constants. *Journal of Geophysical Research*, *85*, 1455–1461. https://doi.org/10.1029/JB085iB03p01455

Yamashita, T., & Ohnaka, M. (1991). Nucleation process of unstable rupture in the brittle regime - a theoretical approach based on experimentally inferred relations. *Journal of Geophysical Research*, *96*(B5), 8351–8367. https://doi.org/10.1029/91JB00106